An Investigation of the Bacterial Communities within a Soil Macroaggregate

Jonathan Y. Lin
Microbial Diversity Course 2017, Marine Biological Laboratory, Woods Hole, MA, USA 02543
Department of Land, Air, and Water Resources, University of California, Davis, CA, USA 95616

Introduction

Microbial ecosystems are multi-scale in nature. While most surveys of environmental microbial communities are performed at broad landscape levels, microbial interactions at microscales are likely to be the dominant drivers of population structure and dynamics affecting global biogeochemical cycles (1). Yet, few studies have investigated the spatial organization of environmental microbial communities at the microscale. These studies are needed to fully understand the roles that biological interactions play in microbial community function (1). Soils are composed of aggregates, structural arrangements formed by particles bound together by organic matter, bacterial polysaccharides, and fungal hyphae (2). Aggregates are separated into different size fractions (0.2 to > 2,000 μm diameter), are hotspots of microbial diversity, and are known to determine soil aeration and drainage (2). Many studies employ bulk soil sampling and homogenization methods, which limit our understanding of the fine-scale physicochemical conditions and spatial patterning of microorganisms in soils. As a result, the structure and function of microbial communities at the soil aggregate level remain uncharacterized. This study represents preliminary attempts to address these shortcomings by investigating the presence of different bacterial communities adapted to different layers of a soil macroaggregate using a combination of molecular and microscopy techniques.

Methods

Soil aggregate collection and fractionation

Soil macroaggregates (≥ 2,000 mm diameter) were collected from an agricultural plot at Coonamessett Farm, East Falmouth, MA, USA (41.68° N, 78.58° W). Soil was passed through a 6.3 mm sieve (Fisher) and the resulting aggregates were stored with wetted paper towels at room temperature until use. 10 aggregates were weighed before and after 3 days of air-drying to calculate the water content.

Soil aggregates were separated into outer, inner, and core sections by using a soil aggregate erosion (SAE) method as described previously (3, 4). Briefly, individual aggregates were weighed, dried, and placed into a plastic container with knurled edges located near the face of the lid. The container was then gently rotated at a consistent pace, causing the aggregate to roll across the inner wall of the container and material to erode off the surface. The eroding aggregate was weighed periodically to determine the proportion of material that had been removed by erosion. When the weight of the aggregate had decreased by ~33% compared to its starting weight, the eroded soil fraction was collected. Each aggregate was fractioned into three ~33% fractions by weight (outer, inner, core) and stored at -20°C until use. Aggregates that broke into multiple fragments before completing the fractionation were removed.

DNA extraction and quantitative PCR

Total DNA from each aggregate fraction was extracted by using the QIAmp Powerfecal DNA isolation kit (Qiagen) and quantified by using the Quantifluor ONE dsDNA assay (Promega). To compare the abundance of denitrifying bacteria in the different aggregate fractions, quantitative PCR (qPCR) was performed using degenerate primers targeting the genes for nitrate reductase (narG), nitrite reductase (nirS), and nitrous oxide reductase (nosZ) (Table 1). The abundance of

the total bacteria determined with general primers targeting the 16S rRNA gene was used as the control (Table 1). Amplification reactions were performed in 20 ul mixtures containing 10 or 1 ng template DNA, 2 µM each primer, and 10 ul of GoTaq qPCR master mix (Promega) using a QuantStudio 5 thermocycler with a melting curve analysis (Applied Biosystems). The annealing temperature used for all primers was 60°C. Due to the absence of a working positive control, the Ct value for each target gene was divided by the Ct value for the 16S rRNA gene in each sample to estimate the relative abundance of denitrifying bacteria.

Table 1. Primers used in this study

Target	Primer	Sequence	Reference
narG	narG F	5'-TCGCCSATYCCGGCSATGTC-3'	Blaud et al, 2017 (5)
	narG R	5'-GAGTTGTACCAGTCRGCSGAYTCSG-3'	
nirS	nirS4Q F	5'-GTSAACGYSAAGGARACSGG-3'	Blaud et al, 2017 (5)
	nirS6Q R	5'-GASTTCGGRTGSGTCTTSAYGAA-3'	
nosZ	nosZ1840 F	5'-CGCRACGGCAASAAGGTSMSSGT-3'	Blaud et al, 2017 (5)
	nosZ2090 R	5'-CAKRTGCAKSGCRTGGCAGAA-3'	
16s rRNA	515F	5'-GTGCCAGCMGCCGCGGTAA-3'	Turner et al, 1999 (6)
	907R	5'-CCGTCAATTCMTTTRAGTTT-3'	

Catalyzed reporter deposition fluorescence in situ hybridization

Catalyzed reporter deposition fluorescence in situ hybridization (CARD-FISH) was performed to visualize the bacterial communities within soil aggregates. 100 mg of soil from each aggregate fraction was fixed overnight in a 2% (v/v) solution of formamide in phosphate-buffered saline. The mixture was then washed twice in PBS and centrifuged at 10,000 g for 1 min. 50 ul of the supernatant was then filtered on a membrane filter, hybridized with horseradish peroxidase (HRP)-labeled probes targeting general bacteria and Betaproteobacteria (Table 2) for 2 hours at 37°C, amplified with tyramide, and stained with DAPI nucleic acid stain. Finished slides were mounted on citifluor vectashield (Vector Laboratories). The fluorescence was visualized with a Zeiss Axiocam A2 microscope with the appropriate filter sets.

Table 2. CARD-FISH probes used in this study

Probe	Target	Sequence	Label
BET42a	Betaproteobacteria	5'-GCTTCCCACTTCGTTT-3'	HRP
EUB338-I-III	Bacteria	5'-GCWGCCWCCCGTAGGWGT-3'	HRP

Aggregate cryosectioning and microscopy

To examine the spatial patterning of bacterial communities inside an aggregate, an attempt was made to embed and thin section soil aggregates for microscopy. Two small aggregates (~75 mm^3) were briefly wetted in sterile deionized water and then embedded in Tissue-Tek OCT solution (Sakura Finetek) at room temperature overnight. Afterwards, the embedded aggregate was submerged in liquid nitrogen and stored at -20°C until use. The aggregate was sliced into 25-60 µm sections using a microtome at the MBL central microscopy core facility, and the thin sections were immediately mounted onto a glass slide. The slides were stained with DAPI nucleic acid stain and mounted on citifluor vectashield (Vector Laboratories) before viewing. The aggregate slices were visualized by bright field and fluorescence microscopy on a Zeiss Axiocam A2 using the appropriate filter sets.

Microelectrode profiling

To determine the concentration of O_2 inside soil aggregates, a Clark-type electrode was used measure the linear shifts of O_2 within the different layers inside an aggregate. A 50 and 100 µm diameter tip size-microsensor was attached to a motorized micromanipulator (Figure 1) connected to a Field MultiMeter 7614 (Unisense). Soil aggregates (~30-75 mm^3) were submerged in sterile deionized water overnight and placed on wetted cotton pads prior to measurement (Figure 1). Vertical profiles were measured in 100 µm steps to a depth of 3,000-10,000 µm starting at 1,000 µm above the surface of the aggregate. Profiles were measured in 5 aggregates, and repeated in one individual aggregate. The probe was programmed and data were collected by using the SensorTrace Pro 2.8.2 software.

Ion chromatography

Nitrate from soil was extracted using deionized water as described previously (7). Briefly, 100 mg of soil from each aggregate fraction was re-suspended in 5 ml of sterile deionized water and vigorously vortexed. The suspension was then centrifuged at 10,000 g for 1 min, the supernatant was sterile filtered using a 0.2 µm filter, and submitted for analysis by ion chromatography (Dionex ICS-2000) using a IonPac AS22 Fast column (Dionex) and IonPac AG22 guard column (Dionex) at 30°C. The solvents used were 1.4 mM $NaHCO_3$ and 4.5 mM Na_2CO_3 (1.2 ml/min).

Results and Discussion

Microelectrode profiles

The average water content was 16%. The O_2 microelectrode profiles revealed the presence of anoxic (0 µmol/L) regions within soil aggregates. Interestingly, the depth of the oxygen gradients varied from 1,000-6,000 µm (Figure 1). In addition, 2 of the aggregates profiled did not possess anoxic regions, which may be correlated with the size of the aggregate (Figure 1). Together, these results show that soil aggregates have variable O_2 gradients with heterogeneous interiors.

Ion chromatography and quantitative PCR

Interestingly, although the extractable nitrate levels were decreased in the aggregate core and inner layers compared to the outer layer, these values were not statistically significant (Figure 2B). For the genes in the denitrification pathway that were tested in this study (Figure 2A), no significant differences in the abundance of narG, nirZ, and nosZ between any of the aggregate layers were detected (Figure 2C-E). These results suggest that, at least using the methods here, the communities of denitrifying bacteria do not differ between the layers of a soil aggregate.

CARD-FISH and microscopy

Soil aggregates were successfully cryosectioned using a microtome apparatus. However, despite an extended overnight incubation, the aggregate centers were not fully embedded with the Tissue Tek OCT medium and fragmented after mounting onto glass slides. As a result, only the outer layer of particles remained attached to the slide, revealing concentric outer rings that were phase-bright when visualized by bright-field microscopy (Figure 3A & B). When stained with DAPI, many soil particles produced autofluorescence, introducing high levels of background noise. Bacterial structures were not identifiable, although large root hairs or fungal hyphae were prominent (Figure 3C & D).

While CARD-FISH successfully revealed the presence of general bacteria in the outer and inner aggregate fractions (Figure 4A-C), no fluorescence was visible from the betaproteobacteria probes. This may be due to an inhibiting artifact introduced during the hybridization procedure. In contrast, both the betaproteobacteria and bacteria-targeting probes produced visible

fluorescence in the aggregate core fraction (Figure 4D-F), revealing their presence in moderate abundance. Unfortunately, due to the high level of background noise, the bacterial morphologies were not easily distinguishable by the microscope camera (Figure 4E).

Methodological challenges are major factors that limit the study of environmental microbial communities at the microscale. For instance, visualization techniques (i.e. FISH) are often limited in high-throughput capacity and are highly sensitive to compounds from environmental samples. Although several of the results from this study were negative, the finding of oxygen gradients that transition from oxic to anoxic regions in soil aggregates is consistent with previous reports (8). This suggests that physicochemical concentrations vary within different areas of a soil aggregate and provides evidence for the presence of distinct microbial communities adapted to these variations. As such, the negative results from this study underscore the above-mentioned technical challenges and acknowledge the need for refined protocols and alternate methods. Targeted isolations, electron microscopy, and 16S rRNA or functional gene sequencing methods represent higher-resolution methods that may provide more success to study bacterial communities within soil aggregates.

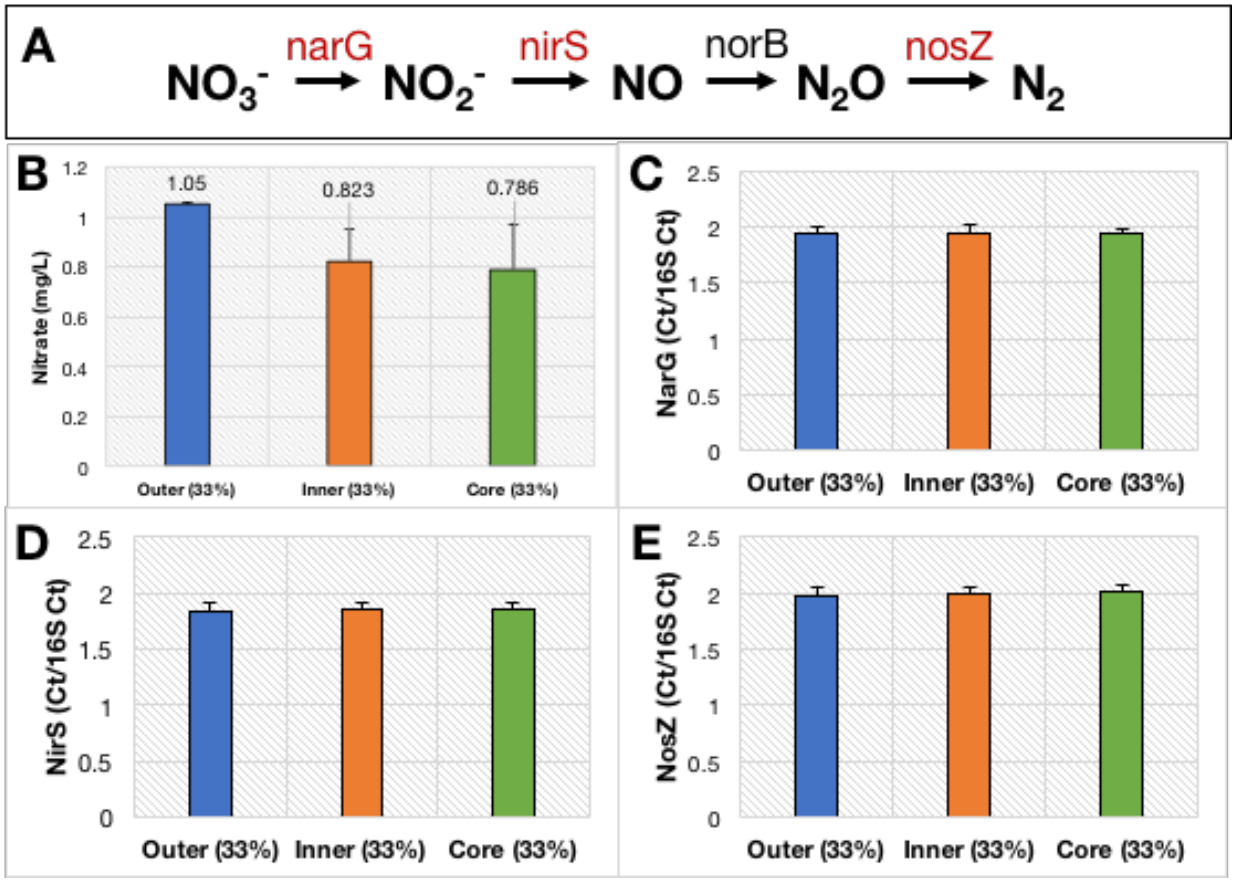

Fig 2. Comparison of nitrate concentrations and estimation of denitrification gene abundance between soil aggregate fractions. (**A**) General overview of the denitrification pathway and the genes involved in each step. Genes quantified in this study are in red. (**B**) Extractable nitrate levels between soil aggregate fractions. Nitrate was extracted using sterile deionized water and quantified by ion chromatography. The abundance of bacterial genes for nitrate reductase (**C**), nitrite reductase (**D**), and nitrous oxide reductase (**E**) between soil aggregate fractions quantified by qPCR. Values are expressed as the ratio of the Ct for the target gene and the Ct for the 16S rRNA gene for each sample (3 replicates).

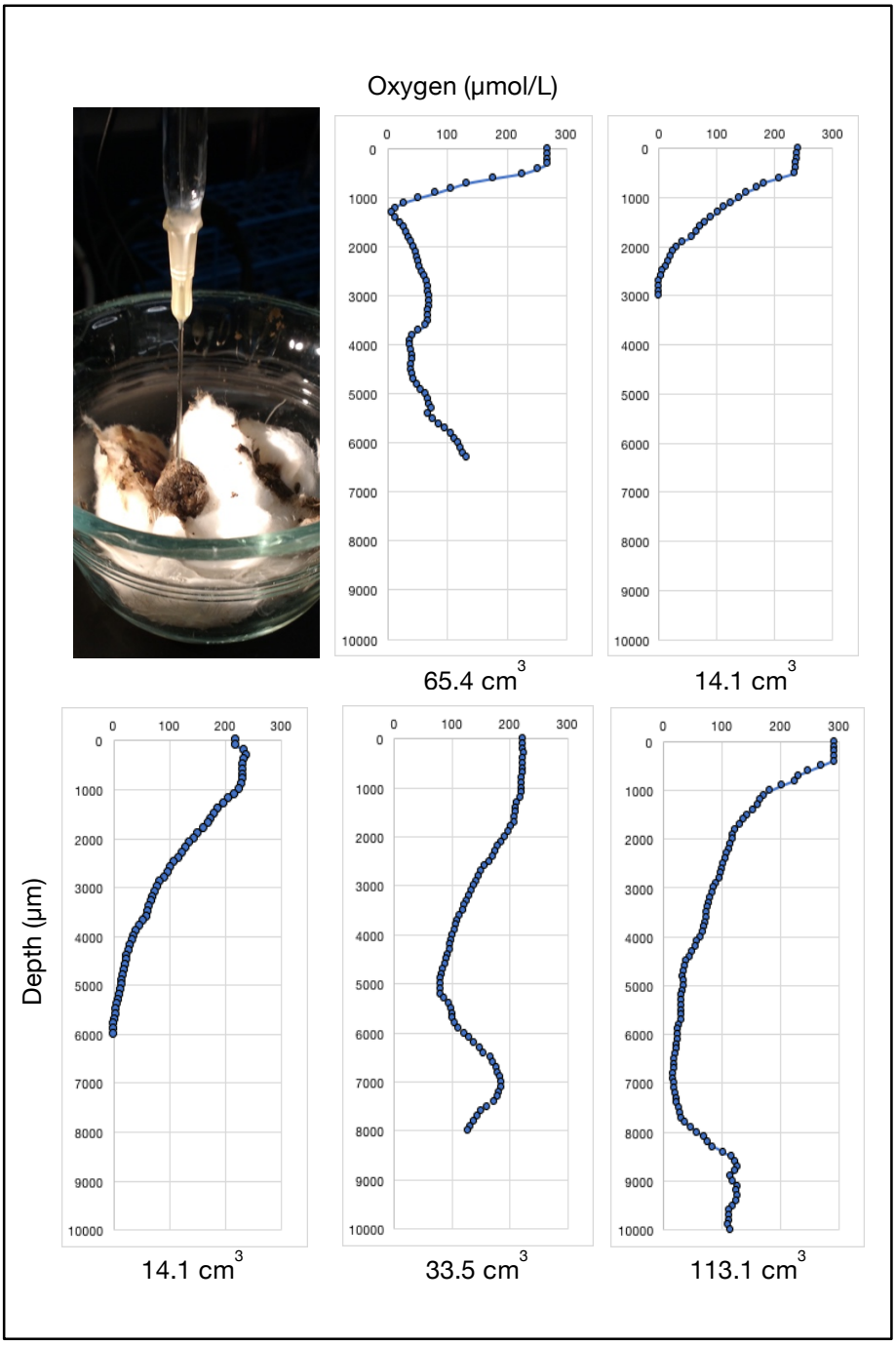

Fig 1. O_2 microelectrode profiles of five soil aggregates. Aggregates were soaked in sterile deionized water overnight prior to profiling. O_2 concentrations were measured with a Clark-type microsensor mounted on a motorized micromanipulator (Top left panel). The approximate volume of each aggregate is displayed below each profile.

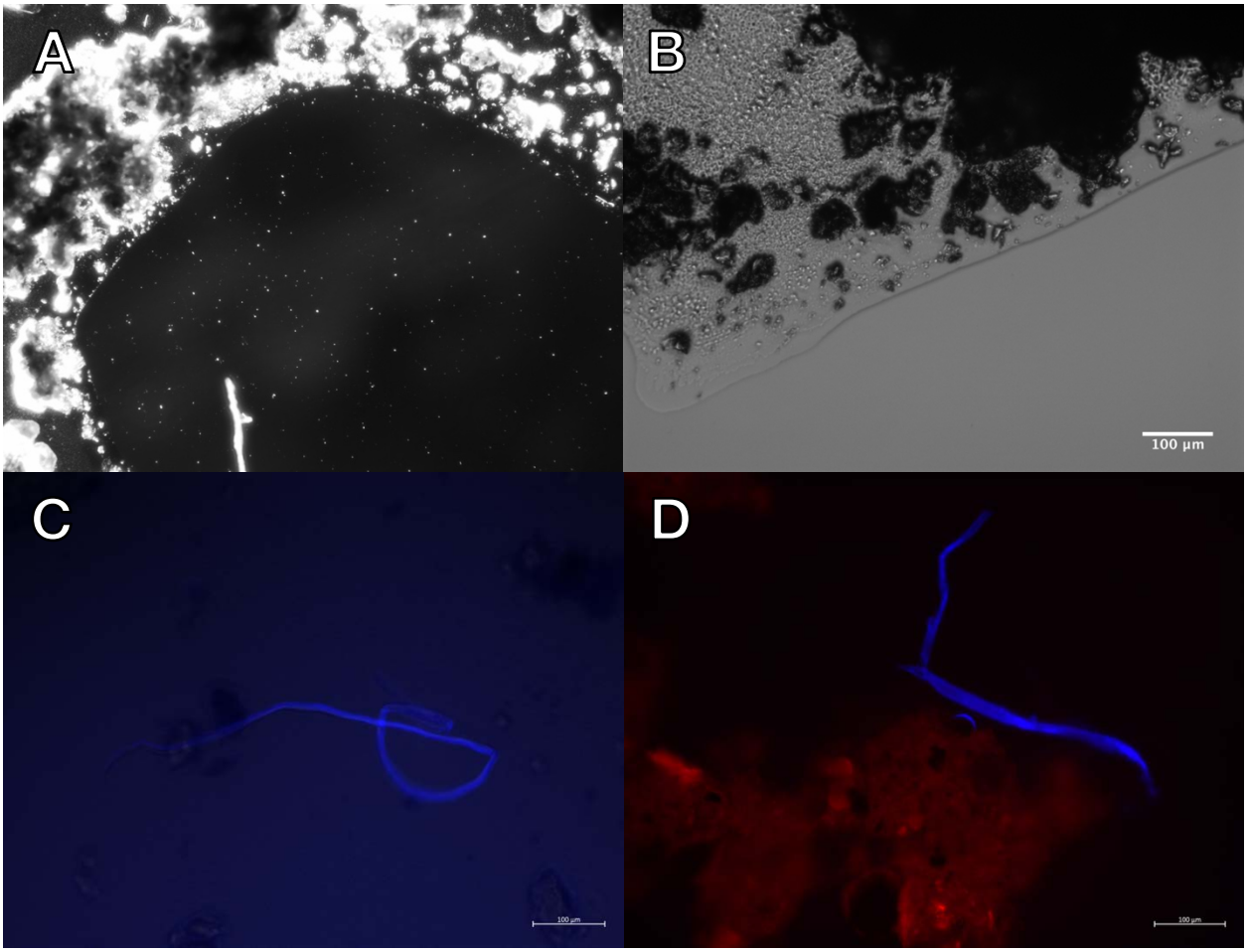

Fig 3. Bright field (**A-B**) and fluorescence (**C-D**) microscopy images of soil aggregate cryosections. Note that many soil particles are phase-bright. Fluorescent images were stained with DAPI nucleic acid stain. Blue, DAPI; Red, autofluorescence; scale bar, 100 µm for all images.

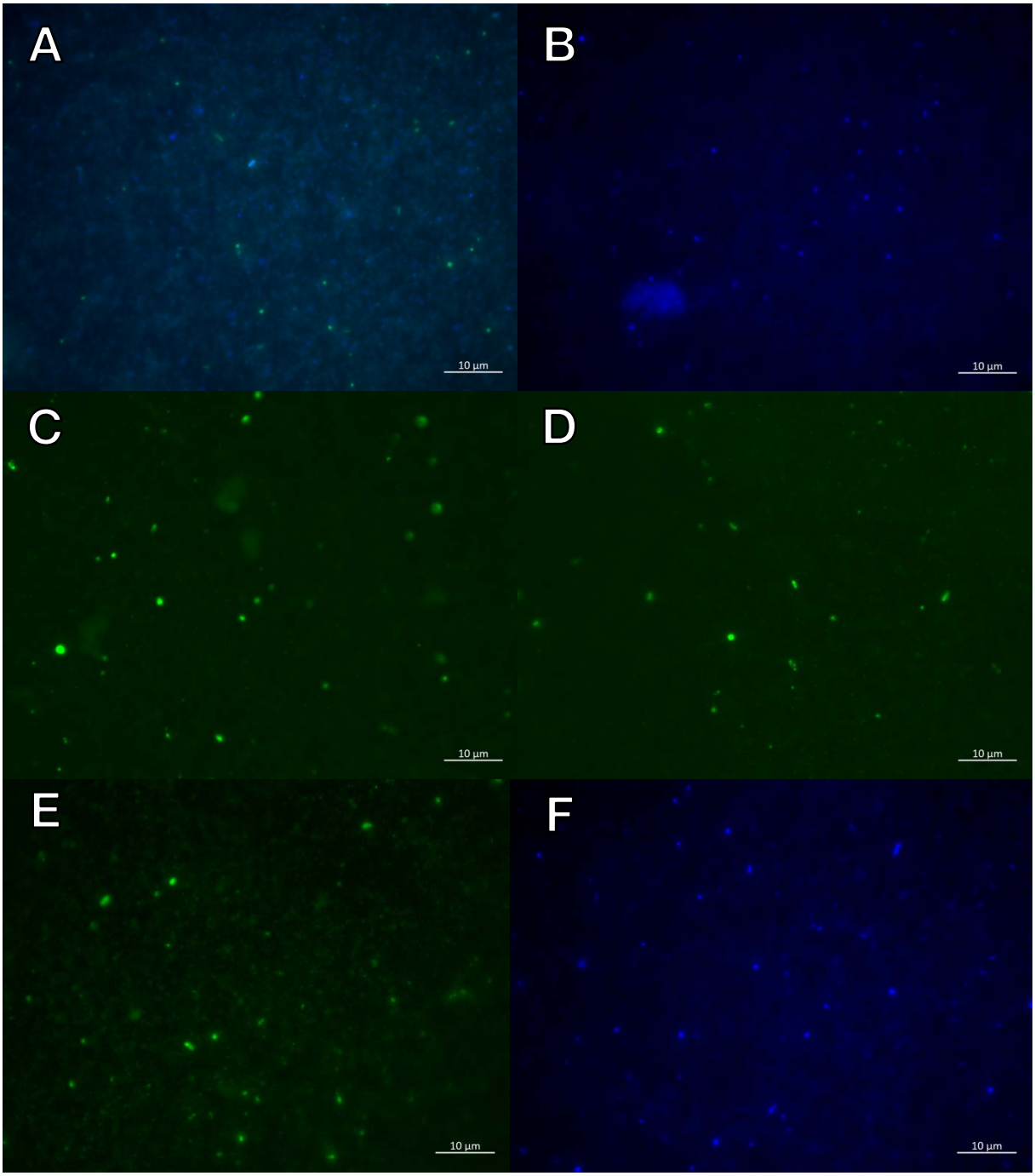

Fig 4. CARD-FISH images of soil aggregate fractions. Fluorescent images of the outer (**A-B**) Green (bacteria), Blue (DAPI); inner (**C**) Green (bacteria); and core (**D**) Green (bacteria); (**E-F**) Green (betaproteobacteria), Blue (DAPI) layers of a soil aggregate.

Side project: Nitrogen fixation by a novel termite gut microaerophile

Introduction

Termites are remarkable for their ability to efficiently degrade lignocellulosic plant material, a process that is mediated by an intricate symbiosis with their gut microbial community (9). The termite gut community is dominated by a diverse set of bacteria, and in the lower termites, protozoan flagellates that inhabit the anoxic (0% O_2) lumen (9). In the microoxic (0.1-10% O_2) periphery, the ecological roles of the less abundant microaerophiles are not well characterized (10). Previous studies have shown that strains from the phylum '*Verrucomicrobia*' isolated from the termite gut under microoxic conditions have genetic capabilities for N_2 fixation, cellulose degradation, and O_2 consumption (11–13). However, the functional capabilities for many of these strains remain uncharacterized. This study attempted to gain a better understanding of the nitrogen utilization strategies in one the uncharacterized strains by testing its ability to fix dinitrogen under microoxic and anoxic conditions.

Methods

Media and cultivation

Opitutaceae bacterium strain TAV5, along with the recently renamed verrucomicrobium *Didymococcus colitermitum* TAV2^T, (11, 14) was previously isolated from the hindgut homogenates of *Reticulitermes flavipes* (Kollar) termites (12). For routine maintenance, strain TAV5 was grown on R2A agar plates (Difco BD) in air at 30ºC and sub-cultured until used for experiments.

For growth experiments, strain TAV5 was grown in a modified minimal broth (M9) containing a trace elements solution, vitamins solution, and glucose and ammonium chloride as the sole carbon and nitrogen sources, respectively (See Appendix I). To test for potential dinitrogen fixing activity, cultures of strain TAV5 were incubated in stoppered anaerobic culture tubes (Chemglass) containing 5 ml M9 broth with and without 18.7 mM ammonium chloride (M9 N-free). The medium was sparged with a mixture of N_2/CO_2 gas (80:20, v/v) and immediately sealed with sterile butyl rubber stoppers. Under a starting headspace of 80:20 N_2/CO_2, some culture tubes were injected with atmospheric air (21% O_2) to obtain a final headspace concentration of 2% O_2. The tubes were shaken at ~200 RPM at 27-28ºC and growth was measured by spectrophotometry at a wavelength of 600 nm.

Acetylene reduction assay

Nitrogenase activity in stationary cultures of strain TAV5 was determined by an acetylene reduction assay. An equal volume of gas in each culture tube was replaced with acetylene gas to obtain a final headspace concentration of 0.1% (v/v) acetylene. Cultures were then shaken at ~200 RPM at 27-28ºC for 3 days, and the concentrations of ethylene and acetylene were measured at regular time intervals on a gas chromatograph (Shimadzu GC-2014). To confirm the presence of N_2-fixing activity by Nitrogenase, 100 ul of 3.7 M ammonium chloride was spiked into several cultures growing in M9 N-free during the experiment to inhibit the enzyme. Due to the absence of a working ethylene standard, the trace occurring before the acetylene peak was inferred to represent ethylene (Figure 6A).

Organic acid analysis

To determine whether strain TAV5 produces short-chain fatty acids (SCFAs) from glucose by fermentation or incomplete oxidation during growth, 1 ml of the culture fluid at stationary phase was removed simultaneously during the growth experiments and stored at -20ºC until analysis.

The culture fluid was centrifuged at 10,000 g for 1 min, the supernatant was removed and filtered through a 0.20 µm filter and acidified by adding 100 ul of 5 N H_2SO4 before analysis. SCFAs and monosaccharides were detected and quantified by high-performance liquid chromatography (Shimadzu LC2010C HT) using an Aminex HPX-87H ion exclusion column (125-0140; Bio-Rad) with a guard cartridge (125-0129; Bio-Rad) at 60°C. Products were detected using a UV/vis detector at a wavelength of 214 nm and the solvent used was 5 mM H_2SO_4 (0.6 ml/min).

Phylogenetic analysis

The complete genome of strain TAV5 was sequenced as described previously (13). Strain TAV5 possesses a single copy of the 16S rRNA gene, the full-length sequence of which was obtained from the genome and used for analysis. The 16S rRNA gene sequence for strain TAV5 and closely related strains from the phylum *Verrucomicrobia* were aligned using MUSCLE (15). Evolutionary distances between strains were determined and phylogenetic analyses were performed in MEGA7 (16).

Results and Discussion

Phylogenetic analysis

Strain TAV5 formed a monophyletic group within the '*Verrucomicrobia*' family *Opitutaceae*, located in the class *Opitutae* (subphylum 4) (Figure 5). Based on the 16S rRNA gene, strain TAV5 shared a 96.7% sequence identity with its closest cultivated neighbor, *Didymococcus colitermitum* TAV2^T. Given that the sequence identity to its cultivated neighbor falls below the 98.65% cutoff typically accepted for species demarcation (17), this strain may represent a novel genus. However, more phylogenetic and phenotypic characterization is needed to confirm the taxonomic position of this strain.

Organic acid analysis and acetylene reduction assay

Strain TAV5 produced measurable amounts of acetate, formate, propionate, and succinate from glucose under both 0% and 2% O_2. However, due to measurements that were significantly higher than the prepared calibration standard, reliable quantifications of glucose could not be obtained. As a result, the molar ratios of glucose to each SCFA produced could not be calculated from the trace data. Strain TAV5 appeared to produce higher concentrations of acetate, formate, and propionate under 2% O_2 than under 0% O_2, suggesting that oxygen may aid in the incomplete oxidation of glucose into these compounds.

Strain TAV5 reduced acetylene under nitrogen-free conditions. When grown in M9 N-free, the acetylene peaks detected by the chromatograph became visibly decreased and was replaced with a putative ethylene trace by 31 hours (Figure 6A). The concentrations of acetylene did not decrease in the cultures of strain TAV5 grown in M9 (nitrogen-containing) or in the uninoculated control (Figure 6B), nor were putative ethylene traces detected in the chromatographs of these samples. Finally, the addition of 100 ul of 3.7 M ammonium chloride to one culture grown in M9 N-free at 31 hours prevented the further reduction of acetylene, inhibiting Nitrogenase activity. Strain TAV5 fixed N_2 under both 2% and 0% O_2 (not shown). These results provide evidence that strain TAV5 can fix N_2 under both microoxic and anoxic conditions. Further analysis of the nitrogen utilizing strategies of strain TAV5, including its *in situ* activity in the termite gut, can now be investigated in future experiments.

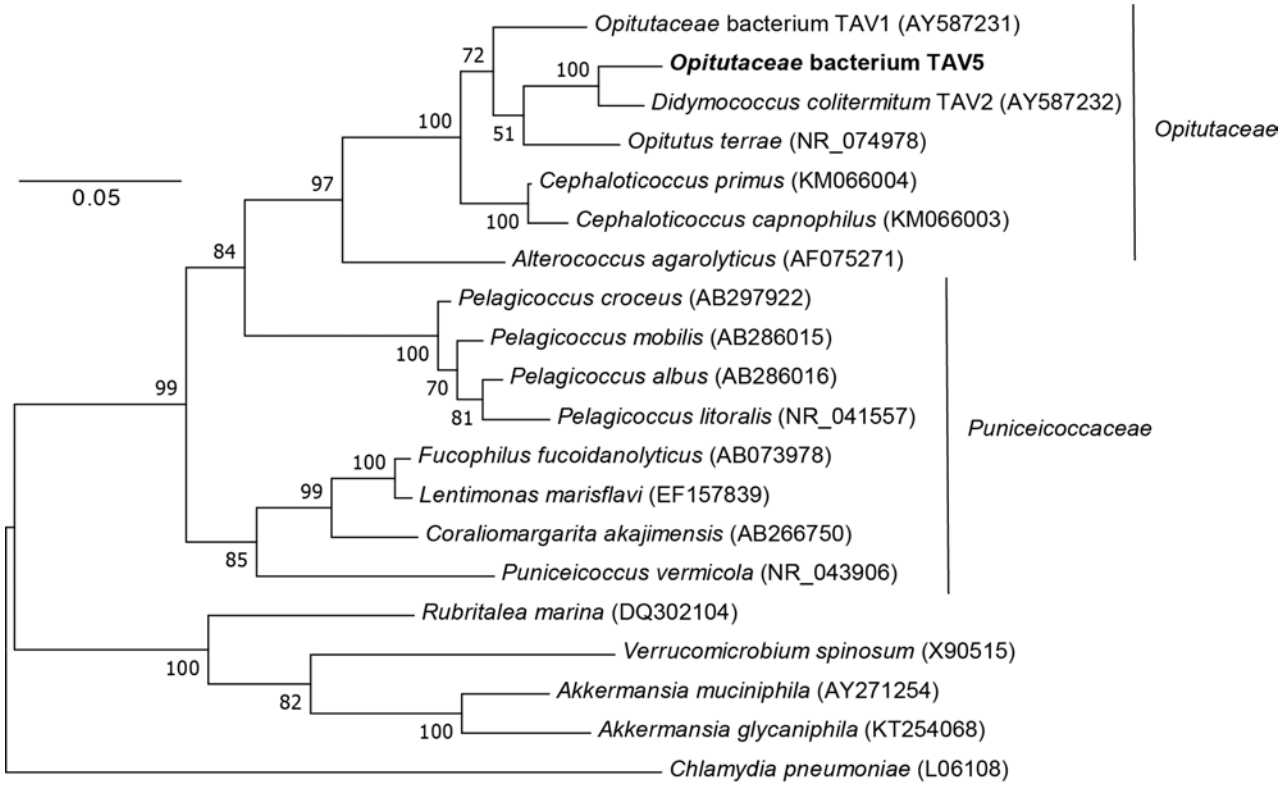

Fig 5. Maximum-likelihood-based 16S rRNA gene phylogeny of strain TAV5. The alignment was generated using MUSCLE. Phylogenetic analysis, including bootstrapping and tree visualization, was performed in MEGA7 using the Tamura-Nei model and nearest neighbor interchange. The phylogeny was based on 1315 shared nucleotide positions and the numbers at branch nodes indicate bootstrap support (500 replicates) above 50%. Other members of the '*Verrucomicrobia*' are given as reference species. Genbank accession numbers are shown in parentheses. Bar, 0.05 changes per nucleotide.

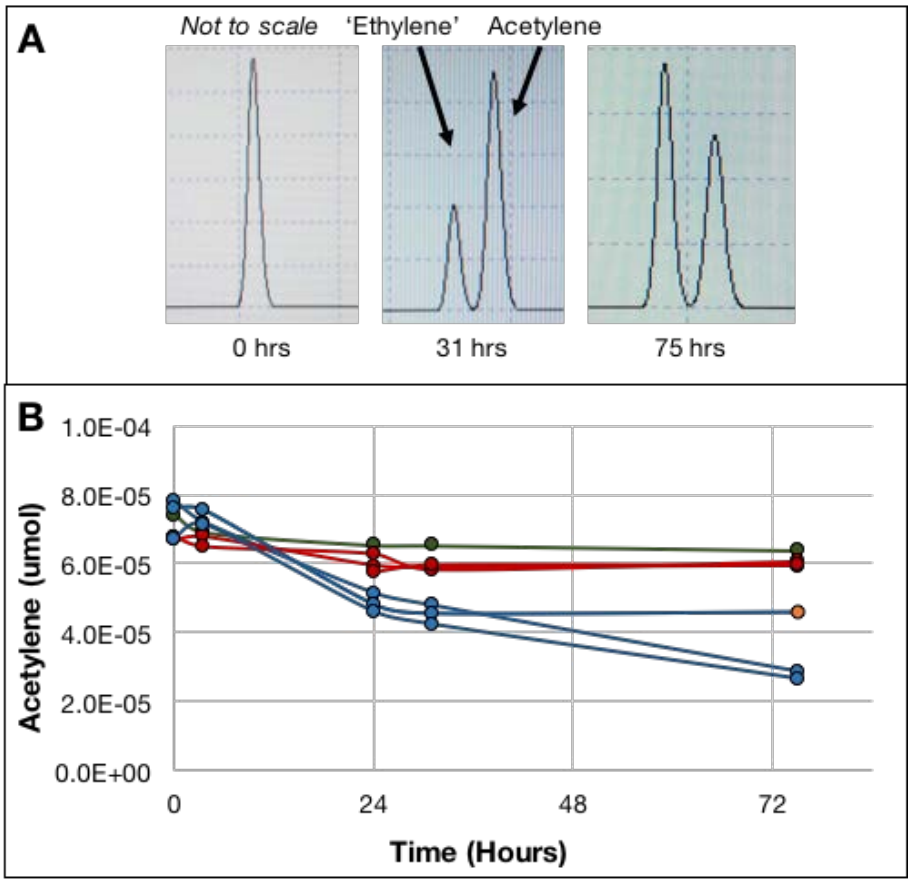

Fig 6. Acetylene reduction assay of TAV5 cultures under microxic (2% O_2) and anoxic (0% O_2) conditions. (**A**) Representative gas chromatograph trace peaks of acetylene and ethylene sampled from culture tubes at 0-75 hours after the amendment of 0.1% acetylene to the headspace. (**B**) The decrease of acetylene by stationary cultures of strain TAV5 from 0-75 hours after the amendment of 0.1% acetylene to the headspace. Blue lines, strain TAV5 in M9 N-free with 2% O_2; Red lines, strain TAV5 in M9 with 0% O_2; Green, uninoculated M9 N-free medium with 2% O_2 control; Orange circle, one culture of strain TAV5 in M9 N-free with 2% O_2 injected with 100 ul of 3.7 M NH_4Cl at 31 hours.

Acknowledgements
I am extremely grateful to the course co-directors (Dianne & Jared) and instructors (Scott Dawson & George O' Toole) for their advice and help. I thank Jared especially for his advice on cultivating termite gut bacteria and for his trace elements 'secret sauce' recipe – which enabled me to finally successfully grow strain TAV5 in a defined, nitrogen-free medium.

This project could not have been possible without the help and guidance from the following teaching assistants: Kyle Costa (Acetylene reduction, qPCR), Scott Saunders (HPLC), Bingran Cheng (Microelectrode, GC), Matthew Tien (PCR), Viola Krukenberg (FISH), and Alicja Dabrowska (IC). I am also grateful for the camaraderie with fellow soil enthusiasts Fatimah Hussain and Samuel Barnett – thank you for fruitful discussions on soil microbiology! Finally, I thank Coonamessett Farm for access and permission for sampling and the Abigail Salyers Endowed Scholarship for funds to attend this course.

References

1. Cordero OX, Datta MS. 2016. Microbial interactions and community assembly at microscales. *Curr Opin Microbiol* **31**:227–234.
2. Rillig MC, Muller LA, Lehmann A. 2017. Soil aggregates as massively concurrent evolutionary incubators. *ISME J*.
3. Blackwood CB, Dell CJ, Smucker AJM, Paul EA. 2006. Eubacterial communities in different soil macroaggregate environments and cropping systems. *Soil Biol Biochem* **38**:720–728.
4. Park E-J, Smucker AJM. 2005. Erosive Strengths of Concentric Regions within Soil Macroaggregates. *Soil Sci Soc Am J* **69**:1912–1921.
5. Blaud A, Menon M, van der Zaan B, Lair GJ, Banwart SA. 2017. Effects of dry and wet sieving of soil on identification and interpretation of microbial community composition, p. 119–142. *In* Sparks, SAB and DL (ed.), *Advances in Agronomy*. Academic Press.
6. Turner S, Pryer KM, Miao VPW, Palmer JD. 1999. Investigating deep phylogenetic relationships among Cyanobacteria and plastids by small subunit rRNA sequence analysis. *J Eukaryot Microbiol* **46**:327–338.
7. Wheatley RE, MacDonald R, Smith AM. 1989. Extraction of nitrogen from soils. *Biol Fertil Soils* **8**:189–190.
8. Sexstone AJ, Revsbech NP, Parkin TB, Tiedje JM. 1985. Direct Measurement of Oxygen Profiles and Denitrification Rates in Soil Aggregates. *Soil Sci Soc Am J* **49**:645–651.
9. Brune A. 2014. Symbiotic digestion of lignocellulose in termite guts. *Nat Rev Microbiol* **12**:168–180.
10. Isanapong J, Sealy Hambright W, Willis AG, Boonmee A, Callister SJ, Burnum KE, Paša-Tolić L, Nicora CD, Wertz JT, Schmidt TM, Rodrigues JL. 2013. Development of an ecophysiological model for *Diplosphaera colotermitum* TAV2, a termite hindgut Verrucomicrobium. *ISME J* **7**:1803–1813.
11. Wertz JT, Kim E, Breznak JA, Schmidt TM, Rodrigues JLM. 2012. Genomic and physiological characterization of the *Verrucomicrobia* isolate *Diplosphaera colitermitum* gen. nov., sp. nov., reveals microaerophily and nitrogen fixation genes. *Appl Environ Microbiol* **78**:1544–1555.
12. Stevenson BS, Eichorst SA, Wertz JT, Schmidt TM, Breznak JA. 2004. New strategies for cultivation and detection of previously uncultured microbes. *Appl Environ Microbiol* **70**:4748–4755.
13. Kotak M, Isanapong J, Goodwin L, Bruce D, Chen A, Han CS, Huntemann M, Ivanova N, Land ML, Nolan M, Pati A, Woyke T, Rodrigues JLM. 2015. Complete genome sequence of the *Opitutaceae* bacterium strain TAV5, a potential facultative methylotroph of the wood-feeding termite *Reticulitermes flavipes*. *Genome Announc* **3**.

14. Wertz JT, Kim E, Breznak JA, Schmidt TM, Rodrigues JLM. 2017. Correction for Wertz et al., "Genomic and physiological characterization of the *Verrucomicrobia* isolate *Didymococcus colitermitum* gen. nov., sp. nov., reveals microaerophily and nitrogen fixation genes." *Appl Environ Microbiol* **83**.
15. Edgar RC. 2004. MUSCLE: multiple sequence alignment with high accuracy and high throughput. *Nucleic Acids Res* **32**:1792–1797.
16. Kumar S, Stecher G, Tamura K. 2016. MEGA7: Molecular evolutionary genetics analysis version 7.0 for bigger datasets. *Mol Biol Evol* **33**:1870–1874.
17. Kim M, Oh H-S, Park S-C, Chun J. 2014. Towards a taxonomic coherence between average nucleotide identity and 16S rRNA gene sequence similarity for species demarcation of prokaryotes. *Int J Syst Evol Microbiol* **64**:346–351.

Appendix I

Modified M9 Salts Broth (Adapted from ATCC 2511)

(Per liter)
Sodium phosphate dibasic (Na_2HPO_4) – 12.8 g
Potassium phosphate dibasic (KH_2PO_4) – 3.0 g
Sodium chloride (NaCl) – 0.5 g
Ammonium chloride (NH_4Cl) – 1.0 g
1000X Trace elements solution – 1 ml
1000X Sodium molybdate solution – 1 ml
Distilled water – 478 ml

Dissolve the above in distilled water and autoclave for 25-30 mins. After cooling to 50°C, add the following filter-sterilized solutions:

20% (w/v) Glucose – 20 ml
1 M Magnesium sulfate ($MgSO_4$) – 2 ml
1 M Calcium chloride ($CaCl_2$) – 0.1 ml
0.5% Thiamine – 0.1 ml
1000X Vitamins solution – 1 ml

Salts will precipitate when added to the solution. Mix thoroughly and store at 4°C. Sterile filter again before adding to incubation tubes.

1000X Trace Elements Solution (From Jared Leadbetter)

(Per liter)
20 mM Hydrochloric acid (HCl) – 1.7 ml
Iron (III) chloride hexahydrate ($FeCl_3 \cdot 6H_2O$) – 2.027 g
Boric acid (H_3BO_3) – 30 mg
Manganese (II) chloride heptahydrate ($MnCl_2 \cdot 4H_2O$) – 100 mg
Cobalt (II) chloride hexahydrate ($CoCl_2 \cdot 6H_2O$) – 190 mg
Nickel (II) chloride hexahydrate ($NiCl_2 \cdot 6H_2O$) – 24 mg
Copper (II) chloride dehydrate ($CuCl_2 \cdot 2H_2O$) – 2 mg
Zinc chloride ($ZnCl_2$) – 68 mg

Sodium selenite (Na_2SeO_3) – 4 mg
Sodium molybdate (Na_2MoO_4) – 30.9 mg

1000X Sodium molybdate solution
(Per liter)
Sodium molybdate (NaMoO4) – 1 g

1000X Vitamins solution (From Jared Leadbetter)
(Per liter, dissolved in MOPS)
10 mM MOPS pH 7.2 – 1,000 ml
Riboflavin – 100 mg
Biotin – 30 mg
Thiamine – HCl – 100 mg
L-Ascorbic acid – 100 mg
d-ca-pantothenate – 100 mg
Folic acid – 100 mg
Nicotinic acid – 100 mg
4-aminobenzoic acid – 100 mg
Pyridoxine-HCl – 100 mg
Lipoic acid – 100 mg
NAD – 100 mg
Thiamine pyrophosphate – 100 mg
Cyanocobalamin – 10 mg